

# Potential Phytochemical Inhibitors of the Coronavirus RNA Dependent RNA Polymerase: A Molecular Docking Study

**Ardra. P**

The Himalaya Drug Company

**Prachi Singh**

The Himalaya Drug Company

**Hariprasad VR**

The Himalaya Drug Company

**Babu UV**

The Himalaya Drug Company

**Mohamed Rafiq**

The Himalaya Drug Company

**Raghavendra Pralhada Rao** (✉ [raghavendra.pr@himalayawellness.com](mailto:raghavendra.pr@himalayawellness.com))

The Himalaya Drug Company

---

## Research Article

**Keywords:** SARS-CoV, SARS-CoV-2, RNA Dependent RNA Polymerase (RdRp), phytochemical compound, molecular docking

**Posted Date:** June 17th, 2020

**DOI:** <https://doi.org/10.21203/rs.3.rs-35334/v1>

**License:** © ⓘ This work is licensed under a Creative Commons Attribution 4.0 International License.

[Read Full License](#)

---

# Abstract

The COVID-19 disease that originated in China by the end of 2019 has now become a pandemic and has affected 216 countries as on 08 June 2020. RNA dependent RNA polymerase (RdRp), the core enzyme in the multiprotein replicase-transcriptase complex of coronaviruses, serves as a classical target for inhibiting the coronavirus infectivity. In this study we performed molecular docking of sixty-nine different phytochemical compounds from various herbs with RdRp of both SARS-CoV-2 and its predecessor SARS-CoV. Our results show that various phytochemical constituents from *Withania somnifera* root extract, *Hyssopus officinalis* and *Camellia sinensis* leaf extract have high binding affinity towards RdRps and are comparable to the small molecule drug remdesivir. Their binding interactions reveal that they bind to the amino acid residues involved in nucleoside triphosphate (NTP) entry and recognition site and metal ion cofactor chelating site of both SARS-CoV-2 and SARS-CoV. Hence they are different from the classical nucleotide analog inhibitors of RdRp. This study paves a quick platform for development of targeted therapy using phytochemicals for COVID-19 and other potential SARS coronavirus related outbreaks in future.

## Introduction

The novel coronavirus outbreak which started in Wuhan province, China, at the end of 2019 has now spread across the globe affecting more than 6.7 million people as on 08 June 2020 (WHO situation report 139). The WHO named this disease as COVID-19 and the causative agent as SARS-CoV-2. The COVID-19 was declared as a global pandemic on 11 March 2020 by WHO. This virus belongs to the same family *Coronaviridae* that caused severe acute respiratory syndrome (SARS) in early 2000's and affected five continents with a lethality of 9.6%<sup>12</sup>. Whole genome sequencing of SARS-CoV-2 reveals that it is a novel betacoronavirus distinct from SARS-CoV and the nucleotide sequence of SARS-CoV-2 showed 79% identity with SARS-CoV<sup>3</sup>.

Coronaviruses (CoVs) are enveloped positive sense single-stranded RNA viruses sized 80–220 nm in diameter with a genome size of around 30kb. Two-thirds portion of the CoV genome from the 5'-end, expresses large replicase polyprotein containing RNA-dependent RNA polymerase and helicase. RdRp is the core enzyme of multiprotein replicase–transcriptase complex (RTC) required for transcription as well as replication of CoVs. RNA synthesis is catalyzed by a multiunit nsp12-nsp8-nsp7 complex where nsp12 exhibit RdRp activity and nsp8 and nsp7 act as the cofactors<sup>4</sup>. The RdRp presents an optimal target with additional attributes of lacking a host homolog and high sequence and structural conservation of active sites. The classical inhibitors for RdRp are nucleotide analogs (NA) for example, remdesivir, which will lead to chain termination of RNA synthesis upon incorporation<sup>5</sup>. CoVs stand out as a particularly challenging case for NA drug design due to the presence of an exonuclease (ExoN) domain capable of excising incorporated NAs and thus providing resistance to many of these available antivirals<sup>6</sup>.

For the development of potential antiviral drug candidates, the natural compounds from various herbs offer a huge repertoire. In this study, we selected some herbs based on Ayurvedic literature. Key phytochemicals of these herbs were identified from research articles exploring their chemistry found in published popular scientific research databases viz. PubMed (<https://www.ncbi.nlm.nih.gov/pmc/>), Google Scholar (<https://scholar.google.com/>) and DOAJ (<https://doaj.org/>). The repurposing of herbs for COVID-19 therapy has an additional advantage that most of these have a long history of traditional safe use and can be positioned in market immediately. Molecular docking of phytochemical constituents was performed against the potential target protein RdRp of SARS-CoV and SARS-CoV-2. Our study result found thirty-seven phytochemical compounds with good docking scores which are comparable to antiviral small molecule inhibitor remdesivir.

## Methods

### Target enzyme preparation:

The RdRp structure of SARS-CoV (PDB ID: 6NUR)<sup>7</sup> and SARS-CoV-2 (PDB ID: 7BTF)<sup>8</sup> were obtained from Protein Data Bank (PDB, <https://www.rcsb.org/>) and saved as PDB file (.pdb). For RdRp, the nsp12 (chain A) was selected and the cofactors (nsp7 (chain C) and nsp8 (chain B, D)) were removed from structure for further processing. AutoDock Tools 1.5.6 was used to prepare the protein targets<sup>9</sup>. Any water molecules or ligands were removed and polar hydrogen atoms and Kollman charges were added to the protein and saved as PDBQT file (.pdbqt). The active site pocket covering the amino acid residues involved in the enzyme activity was selected and grid box was placed on it. Cartesian coordinates (x,y,z) of grid box for each protein is saved for input during docking.

### Ligand preparation:

The 3D coordinates of the phytochemicals and positive controls were obtained from PubChem (<https://pubchem.ncbi.nlm.nih.gov/>) in SDF file (.sdf) and were converted to PDB file (.pdb) using Open Babel GUI tool<sup>10</sup>. The ligands were prepared by adding gasteiger charges, merging non-polar hydrogen and setting torsion root and then converted to PDBQT (.pdbqt) files using AutoDock Tools 1.5.6 and saved.

### Docking and visualization:

Docking experiments were performed with sixty nine phytochemical constituents from the herbs using AutoDock Vina 1.1.2 software<sup>11</sup>. The default exhaustiveness value of 8 is given throughout this study. The known drug candidate Remdesivir is used as positive control for docking RdRp. The Gibbs free energy of binding ( $\Delta G$ ) expressed in kcal/mol represents the efficiency of ligand binding to the designated receptor active site and was obtained as a result from AutoDock Vina. Also, the output file of optimal ligand conformations and their interaction with receptor residues were visualized using Biovia Discovery Studio 2.0.1 software.

## Calculation of dissociation constant $K_i$ :

The  $\Delta G$  value obtained from AutoDock Vina is the free energy of binding of ligand to protein. The dissociation constant for protein ligand binding ( $K_i$ ) (in unit of M) can be defined as

$$K_i = \frac{[P][L]}{[PL]} = \frac{1}{K_b}$$

Where  $K_b$  (in unit of  $M^{-1}$ ) is the equilibrium constant for ligand binding,  $[P]$ ,  $[L]$  and  $[PL]$  are equilibrium concentrations of protein, ligand and protein-ligand complex respectively. Therefore, the fast binding rate accompanied by a slow dissociation rate will give a high binding affinity. As we know the free energy of binding can be calculated as

$$\Delta G = -RT \ln K_b \text{ or } \Delta G = RT \ln K_i$$

Where,  $R$  is the universal gas constant ( $1.987 \text{ cal} \cdot \text{K}^{-1} \cdot \text{mol}^{-1}$ ),  $T$  is the temperature in degrees of Kelvin (298.15 K).  $K_i$  values for the potent phytochemical were calculated from the  $\Delta G$  values as follows:

$$K_i = e^{\frac{\Delta G + 1000}{RT}}$$

The dissociation constant for enzyme inhibitor binding ( $K_i$ ) calculated from the free energy data gives the apparent binding efficiency of ligand to receptor active site. Equation makes it apparent that the lower the dissociation constant  $K_i$ , the more negative the standard free energy of binding, indicating that the kinetic parameters determine the thermodynamic properties of the complex, i.e., the stability of the complex and the binding affinity between the protein and ligand<sup>1213</sup>.

## Results And Discussion

### Design of ligand binding pocket of RdRp:

The nsp12 domain is an RNA dependent RNA polymerase which plays pivotal role in catalyzing the RNA replication of coronavirus. The overall architecture of SARS-CoV-2 nsp12-nsp8-nsp7 complex is very similar to that of SARS-CoV with a Root Mean Square Deviation (RMSD) value of 0.82. Analysis of sequence conservation across the coronavirus family reveals that the template entry, template-primer exit, and NTP tunnels, as well as the polymerase-active site, are the most highly conserved surfaces on nsp12<sup>1415</sup>. The superimposed images of RdRp structures 7BTF (SARS-CoV-2) and 6NRU (SARS-CoV) with conserved amino acid residues are shown in **Figure 1**. In the current study we targeted the NTP entry pocket and metal ion stabilizing triad and NTP binding and positioning residues as a possible site for ligand binding there by disrupting the RNA synthesis mechanism of RdRp. The grid box for docking was assigned to these conserved residues for both SARS-CoV and SARS-CoV-2.

## Non-nucleotide analogs as RdRp inhibitors:

The classical drug candidates for RdRps are NAs and many such molecules are under various stages of development. One of the main hurdles in using NAs is the presence of proofreading and exonuclease activity for both SARS-CoV and SARS-CoV-2 in its nsp14 domain (ExoN) <sup>16</sup>. There are also two reported mutations in sub-domain of the nsp12 RdRp (F480L and V557L SARS-CoV numbering). Neither of the resistance mutations directly impact the catalytic site nor substrate-binding pocket, but rather cause minor structural alterations which likely impact an NTP 'checking step' performed by the polymerase before catalysis <sup>17</sup>. These factors increase the fidelity of RNA synthesis by SARS-CoV and thus pose a threat to the use of NAs as possible inhibitors for RdRps. In this study we explored the potential of phytochemicals from common medicinal herbs as non-nucleotide analog inhibitors for both SARS-CoV and SARS-CoV-2 RdRp. Sixty nine active constituents were selected from herbal extracts like *Withania somnifera* root extract, *Hyssopus officinalis*, *Glycyrrhiza glabra* root extract, *Ocimum sanctum* aerial part extract, *Camellia sinensis* leaf extract, *Prunella vulgaris*, *Hedychium spicatum* rhizome extract, *Cyperus scariosus*, *Nigella sativa* seed extract and Triphala fruit and fruit rind extract based on literature.

## Molecular docking of phytochemical compounds:

AutoDock Vina results represent the docking scores as Gibbs free energy of binding ( $\Delta G$  (kcal/mol)) which approximates the sum of all interactions ligand/receptor minus desolvation energies. The docking scores of phytochemicals against both SARS-CoV-2 and SARS-CoV are given in **Table 1**. The control drug molecule remdesivir was shown to have docking scores of -7.2 kcal/mol and -7.5 kcal/mol against RdRp of SARS-CoV-2 and SARS-CoV respectively. Our results showed that thirty seven phytochemicals had  $\Delta G$  values less than the cut-off value -6 kcal/mol and hence they were considered to be potential inhibitors <sup>18</sup>. The dissociation constant for protein ligand binding ( $K_i$ ) were calculated for thirty-seven potent phytochemical compounds and remdesivir and the data is given in **Table 2** in their order of decreasing potency. Many of the phytochemicals in our study showed lower  $K_i$  values than remdesivir, with the  $K_i$  values for later being 5.048  $\mu\text{M}$  and 3.037  $\mu\text{M}$  for SARS-CoV-2 and SARS-CoV respectively. As discussed earlier, lower the  $K_i$  value better the inhibitor. The predicted  $K_i$  values calculated here gives an approximate estimation of the potency of inhibitors and caution should be exercised in extrapolating this data because the experimental  $K_i$  values can be different from the predicted values depending on various biophysical parameters involved in enzyme inhibition <sup>19</sup>.

In our study, lowest docking scores for both SARS-CoV-2 (-9 to -7.7 kcal/mol) and SARS-CoV (-9.3 to -7.8 kcal/mol) were obtained for the phytochemicals from *Withania somnifera* root extract such as withaferin A, withanolide A, B, D,E and F, withasomniferol A, B and C and withanone. These phytochemicals also exhibited the least of the  $K_i$  values among all the phytochemical compounds tested. *Withania somnifera*, commonly known as Ashwagandha, is well established traditionally as a promoter of longevity, well-being, and disease prevention. Some constituents of Ashwagandha have reported anti-influenza properties and are also being prospected *in silico* against COVID-19 <sup>20,21</sup>. Ashwagandha extracts have been shown to inhibit the viral RNA replication by inducing nitric oxide in vitro. It is reported that NO

induction can inhibit RdRps of viruses and can be used as a potential therapy<sup>22,23</sup>. Our results suggest that in addition to its immunomodulatory activity, Ashwagandha can be positioned as anti-viral herbal supplement against COVID-19.

Another medicinal herb with most phytoconstituents displaying potential inhibition was *Hyssopus officinalis* (Hyssop) with  $\Delta G$  values in the range of -8.4 to -7.7 kcal/mol for SARS-CoV-2 and -8.7 to -7.7 kcal/mol for SARS-CoV. This herb is well known for its anti-microbial, anti-fungal, antiviral and immunomodulatory activities and has been shown to possess anti-HIV and anti-HSV activities<sup>24-26</sup>. The major constituent luteolin has been reported to inhibit RNA synthesis in Enterovirus 71 and Coxsackievirus A16<sup>27</sup>. There are no reported studies on inhibition of RdRps by the phytochemical constituents of Hyssop. The flavonoid glycoside diosmin showed the maximum potency with docking scores of -8.4 kcal/mol and -8.7 kcal/mol.

The polyphenols catechins and its isomers from *Camellia sinensis* leaf extract showed good docking scores against both the CoVs in our study. The antiviral activity of catechins is evaluated against many viruses and the major mode of action is inhibition of RNA replication<sup>28</sup>. In our study, epigallocatechin gallate (EGCG) gave the lowest binding energy (-8.3 kcal/mol for SARS-CoV-2 and -8.5 kcal/mol for SARS-CoV) amongst the catechins and this is in line with the literature report that EGCG potentially inhibits the viral replication in vitro when compared to other catechins<sup>29</sup>.

The phytochemicals oleanolic acid and ursolic acid have been reported to exhibit anti-Hepatitis C virus (HCV) activity by acting as noncompetitive inhibitors of HCV NS5B RdRp<sup>29-31</sup>. In our study also, these two molecules sourced from herbs *Prunella vulgaris* and *Ocimum sanctum* aerial part extract showed good affinity towards both SARS-CoV and SARS-CoV-2 RdRp. In addition, several other molecules from different herbs showed moderate docking scores and  $K_i$  values against RdRp.

### **Interaction profile of phytochemical compounds and RdRp – molecular visualization:**

The 3D and 2D visualization of the interaction of nine phytochemicals showing highest binding affinities (low  $K_i$  values) and control drug remdesivir for SARS-CoV-2 is given in **Figure 2**. Similarly, the 2D and 3D visualization of interactions of phytochemicals and remdesivir with SARS-CoV are depicted in **Figure 3**. Most of the phytochemicals have at least one hydrogen bond forming interaction with the residues Lys545-Arg553-Arg555 of NTP entry site and Asp760-Asp761-Asp618 of the  $Mg^{2+}$  ion chelating site. The 2D illustration also depicts the non-bonded interactions like van der Waals forces, pi-cation, pi-alkyl etc. between phytochemicals and amino acid residues Asp623 and Asn691, Thr680, Ser682 and Thr687 (involved in NTP recognition and positioning). The control drug remdesivir is a nucleotide analog that binds to RdRp in similar way as a nucleotide and then leads to chain termination. The interaction of various amino acid residues with remdesivir is discussed in literature<sup>32</sup>. The ligand binding profile of the highest ranked phytochemicals in our screening is in line with the study of Yin et al. for FDA approved antiviral agents like remdesivir, ribavirin and favipiravir<sup>33</sup>.

## Conclusion

The COVID-19 pandemic has infected the whole world in an unprecedented manner and developing a vaccine or other successful pharmacological interventions are the prime need of the hour. Currently there is no system of medicine that has evidence-based treatment for COVID-19 yet various clinical interventions are on trial worldwide. In this pressing situation, the scientific community is considering pluralistic knowledge systems available globally to combat the disease. The herbal medicine system has gained focus globally in providing interventions to combat this pandemic<sup>34,35</sup>. In this context we performed an *in-silico* prospecting of phytochemicals identified from common herbs used in Ayurvedic system of medicine to repurpose against coronavirus infection. The target chosen here namely RdRp is one of the most investigated coronavirus targets and its potential inhibitor, remdesivir, is currently in Phase III clinical trials for establishing its safety and efficacy<sup>36</sup>. In our study, we have identified few phytochemicals from different herbs like *Withania somnifera* root extract, *Hyssopus officinalis*, *Camellia sinensis* leaf extract, *Prunella vulgaris*, *Ocimum sanctum* aerial part extract etc. that have potential to inhibit RdRp from both SARS-CoV and SARS-CoV-2. Further *in vitro*, *in vivo* and clinical studies are warranted to establish the complete pharmacological profile of these molecules. The broad-spectrum activity of these molecules against both the CoVs proves that they can be repurposed even in case of a related coronavirus outbreak in future as well.

## Abbreviations

World Health Organization (WHO), Coronavirus Disease 2019 (COVID-19), Coronavirus (CoV), Severe Acute Respiratory Syndrome Coronavirus-2 (SARS-CoV-2), RNA dependent RNA polymerase (RdRp), non-structural protein (nsp), Nucleotide/nucleoside triphosphate (NTP).

## Declarations

**Acknowledgements:** Authors sincerely thank Dr. Gopu Madhavan, Dr. Shruthi Bhat, R&D Himalaya Drug Company for their inputs and critical evaluation of the manuscript.

**Authors' contribution:** RPR and MR were involved in study designing. AP and PS conducted the *in-silico* work. HVR, UVB were involved in short listing the herbs and respective phytochemicals. AP and RPR wrote the manuscript.

**Declaration of interest:** No potential conflict of interest was reported by the authors.

**Funding information:** The research work was supported by The Himalaya Drug Company, Bengaluru, India.

## References

1. World Health Organization (WHO). Novel Coronavirus ( 2019-nCoV ) Situation Report - 1 21 January 2020. *WHO Bull.* (2020);1.
2. Park SE. Epidemiology, virology, and clinical features of severe acute respiratory syndrome-coronavirus-2 (SARS-COV-2; Coronavirus Disease-19). *Vol. 63, Korean Journal of Pediatrics. Korean Pediatric Society*; 2020. p. 119–24.
3. Ren L-L, Wang Y-M, Wu Z-Q, Xiang Z-C, Guo L, Xu T, et al. Identification of a novel coronavirus causing severe pneumonia in human. *Chin Med J (Engl)*. 133,(2020);1015.
4. Subissi L, Posthuma CC, Collet A, Zevenhoven-Dobbe JC, Gorbalenya AE, Decroly E, et al. One severe acute respiratory syndrome coronavirus protein complex integrates processive RNA polymerase and exonuclease activities. *Proc Natl Acad Sci U S A*. 111,(2014);E3900.
5. Wang M, Cao R, Zhang L, Yang X, Liu J, Xu M, et al. Remdesivir and chloroquine effectively inhibit the recently emerged novel coronavirus (2019-nCoV) in vitro. *Cell Res*. 30,(2020);269.
6. Shannon A, Le NTT, Selisko B, Eydoux C, Alvarez K, Guillemot JC, et al. Remdesivir and SARS-CoV-2: Structural requirements at both nsp12 RdRp and nsp14 Exonuclease active-sites. *Antiviral Res [Internet]*. 178,(2020);104793. Available from: <https://doi.org/10.1016/j.antiviral.2020.104793>
7. Kirchdoerfer RN, Ward AB. Structure of the SARS-CoV nsp12 polymerase bound to nsp7 and nsp8 co-factors. *Nat Commun [Internet]*. 10,(2019);1. Available from: <http://dx.doi.org/10.1038/s41467-019-10280-3>
8. Gao Y, Yan L, Huang Y, Liu F, Zhao Y, Cao L, et al. Structure of the RNA-dependent RNA polymerase from COVID-19 virus. *Science (80- )*. 368,(2020);779.
9. Goodsell DS, Olson AJ. Automated docking of substrates to proteins by simulated annealing. *Proteins Struct Funct Bioinforma*. 8,(1990);195.
10. O'Boyle NM, Banck M, James CA, Morley C, Vandermeersch T, Hutchison GR. Open Babel: An Open chemical toolbox. *J Cheminform*. 3,(2011);33.
11. Trott O, Olson AJ. AutoDock Vina: Improving the speed and accuracy of docking with a new scoring function, efficient optimization, and multithreading. *J Comput Chem*. 31,(2009);NA.
12. Shityakov S, Broscheit J, Förster C.  $\alpha$ -Cyclodextrin dimer complexes of dopamine and levodopa derivatives to assess drug delivery to the central nervous system: ADME and molecular docking studies. *Int J Nanomedicine*. 7,(2012);3211.
13. Du X, Li Y, Xia Y-L, Ai S-M, Liang J, Sang P, et al. Insights into Protein–Ligand Interactions: Mechanisms, Models, and Methods. *Int J Mol Sci*. 17,(2016);144.
14. Gordon CJ, Tchesnokov EP, Woolner E, Perry JK, Feng JY, Porter DP, et al. Remdesivir is a direct-acting antiviral that inhibits RNA-dependent RNA polymerase from severe acute respiratory syndrome coronavirus 2 with high potency. *J Biol Chem*. (2020);jbc. RA120.013679.
15. Gaurav A, Al-Nema M. Polymerases of coronaviruses: Structure, function, and inhibitors. *In: Viral Polymerases: Structures, Functions and Roles as Antiviral Drug Targets. Elsevier*; 2018. p. 271–300.

16. Pachetti M, Marini B, Benedetti F, Giudici F, Mauro E, Storici P, et al. Emerging SARS-CoV-2 mutation hot spots include a novel RNA-dependent-RNA polymerase variant. *J Transl Med [Internet]*. 18, (2020);1. Available from: <https://doi.org/10.1186/s12967-020-02344-6>
17. Ogando NS, Ferron F, Decroly E, Canard B, Posthuma CC, Snijder EJ. The Curious Case of the Nidovirus Exoribonuclease: Its Role in RNA Synthesis and Replication Fidelity. *Vol. 10, Frontiers in Microbiology. Frontiers Media S.A.*; 2019. p. 1813.
18. Shityakov S, Foerster C. In silico predictive model to determine vector-mediated transport properties for the blood&ndash;brain barrier choline transporter. *Adv Appl Bioinforma Chem*. 7,(2014);23.
19. Darras FH, Pang YP. On the use of the experimentally determined enzyme inhibition constant as a measure of absolute binding affinity. *Biochem Biophys Res Commun [Internet]*. 489,(2017);451. Available from: <http://dx.doi.org/10.1016/j.bbrc.2017.05.168>
20. Srivastava AK, Kumar A, Misra N. On the Inhibition of COVID-19 Protease by Indian Herbal Plants: An In Silico Investigation. :1.
21. Cai Z, Zhang G, Tang B, Liu Y, Fu X, Zhang X. Promising Anti-influenza Properties of Active Constituent of *Withania somnifera* Ayurvedic Herb in Targeting Neuraminidase of H1N1 Influenza: Computational Study. *Cell Biochem Biophys*. 72,(2015);727.
22. Ganguly B, Umapathi V, Rastogi SK. Nitric oxide induced by Indian ginseng root extract inhibits Infectious Bursal Disease virus in chicken embryo fibroblasts in vitro. *J Anim Sci Technol*. 60, (2018);4.
23. Takhampunya R, Padmanabhan R, Ubol S. Antiviral action of nitric oxide on dengue virus type 2 replication. *J Gen Virol*. 87,(2006);3003.
24. Fathiazad F, Hamedeyazdan S. A review on *Hyssopus officinalis* L: Composition and biological activities. *African J Pharm Pharmacol*. 5,(2011);1959.
25. Allahverdiyev AM, Bagirova M, Yaman S, Koc RC, Abamor ES, Ates SC, et al. Development of New Antiherpetic Drugs Based on Plant Compounds [Internet]. *Fighting Multidrug Resistance with Herbal Extracts, Essential Oils and their Components. Elsevier*; 2013. 245–259 p. Available from: <http://dx.doi.org/10.1016/B978-0-12-398539-2.00017-3>
26. Kreis W, Kaplan MH, Freeman J, Sun DK, Sarin PS. Inhibition of HIV replication by *Hyssopus officinalis* extracts. *Antiviral Res*. 14,(1990);323.
27. Xu L, Su W, Jin J, Chen J, Li X, Zhang X, et al. Identification of luteolin as enterovirus 71 and coxsackievirus A16 inhibitors through reporter viruses and cell viability-based screening. *Viruses*. 6, (2014);2778.
28. Xu J, Xu Z, Zheng W. A review of the antiviral role of green tea catechins. *Molecules*. 22,(2017);1.
29. Song J-M, Lee K-H, Seong B-L. Antiviral effect of catechins in green tea on influenza virus. *Antiviral Res*. 68,(2005);66.
30. Kong L, Li S, Liao Q, Zhang Y, Sun R, Zhu X, et al. Oleanolic acid and ursolic acid: Novel hepatitis C virus antivirals that inhibit NS5B activity. *Antiviral Res [Internet]*. 98,(2013);44. Available from: <http://dx.doi.org/10.1016/j.antiviral.2013.02.003>

31. Kong L, Li S, Han X, Xiang Z, Fang X, Li B, et al. Inhibition of HCV RNA-dependent RNA polymerase activity by aqueous extract from Fructus Ligustri Lucidi. *Virus Res.* 128,(2007);9.
32. Elfiky AA. Ribavirin, Remdesivir, Sofosbuvir, Galidesivir, and Tenofovir against SARS-CoV-2 RNA dependent RNA polymerase (RdRp): A molecular docking study. *Life Sci.* 253,(2020);117592.
33. Yin W, Mao C, Luan X, Shen D-D, Shen Q, Su H, et al. Structural Basis for the Inhibition of the RNA-Dependent RNA Polymerase from SARS-CoV-2 by Remdesivir. *bioRxiv.* (2020);2020.04.08.032763.
34. Rastogi S, Pandey DN, Singh RH. COVID-19 Pandemic: A pragmatic plan for Ayurveda Intervention. *J Ayurveda Integr Med [Internet].* (2020); Available from: <https://doi.org/10.1016/j.jaim.2020.04.002>
35. Patwardhan B, Chavan-Gautam P, Gautam M, Tillu G, Chopra A, Gairola S, et al. Ayurveda rasayana in prophylaxis of COVID-19. *Comment Curr Sci.* 118,(2020);
36. Wang Y, Zhang D, Du G, Du R, Zhao J, Jin Y, et al. Remdesivir in adults with severe COVID-19: a randomised, double-blind, placebo-controlled, multicentre trial. *Lancet.* 395,(2020);1569.

## Tables

**Table 1:** Docking scores of phytoactive compounds to SARS-CoV and SARS-CoV-2 RdRp (represented as Gibbs free energy change of binding ( $\Delta G$ ) (kcal/mol)). The  $\Delta G$  values in bold represents the values below the cut-off of -6 kcal/mol.

Herb	Phytoactive compounds	PubChem ID	ΔG kcal/mol	
			SARS-CoV-2 (7BTF)	SARS-CoV (6NUR)
<i>Withania somnifera</i> root extract	Withaferin A	265237	-8.5	-9.2
	Withanolide A	11294368	-8.8	-9.1
	Withanolide B	14236711	-7.7	-7.8
	Withanolide D	161671	-9	-9.3
	Withanolide E	301751	-8.6	-8.7
	Withanolide F	135887	-8.4	-8.9
	Withanone	21679027	-8.3	-7.9
	Withasomniferol A	101710595	-8.1	-8.2
	Withasomniferol B	101710596	-8.6	-8.6
	Withasomniferol C	101710597	-8.9	-9
<i>Hyssopus officinalis</i>	Apigenin	5318517	-7.6	-7.8
	Apigenin 7-O-b-glucuronide	5385553	-8.4	-8.6
	Apigenin, 7-.beta.-D-glucopyranoside	5319484	-8	-7.7
	Diosmin	5281613	-8.4	-8.7
	Luteolin	5280445	-7.7	-8
	Luteolin 7-O-beta-d-glucopyranoside	13093777	-8.2	-8.1
<i>Glycyrrhiza glabra</i> root extract	Glycyrrhetic acid	10114	-7.9	-8.1
<i>Ocimum sanctum</i> aerial part extract	Oleanolic acid	10494	-7.6	-7.9
	Ursolic acid	64945	-7.7	-7.6
<i>Camellia sinensis</i> leaf extract	Epicatechin	72276	-6.8	-7.1
	Epicatechin gallate	107905	-8.2	-7.6
	Epigallocatechin	72277	-7.4	-7.3
	Epigallocatechin gallate	65064	-8.3	-8.5
	Gallocatechin	65084	-6.5	-7.3
Triphala fruit & fruit rind extract	Ellaigic acid	5281855	-7.2	-8.2
	Gallic acid	370	-5.8	-5.7
<i>Prunella vulgaris</i>	beta-Amyrenone	12306160	-7.9	-8.4
	beta-Amyrin	73145	-7.8	-8.4
	Betulinic acid	64971	-7.7	-7.6
	Oleanolic acid	10494	-7.6	-7.9
	Ursolic acid	64945	-7.7	-7.6
	Uvaol	92802	-7.6	-7.5
<i>Hedychium spicatum</i> rhizome extract	(E)-beta-Ocimene	5281553	-4.6	-4.7
	(E)-Caryophyllene	5281515	-5.7	-6.2
	1,8-Cineole	2758	-4.8	-5.2
	10-epi gamma Eudesmol	6430754	-6.3	-6.2
	beta-Farnasene	5281517	-5	-5.5
	Caryophyllene oxide	1742210	-6	-6.2
	Cubebol	11276107	-5.7	-6
	Curzerene	572766	-5.6	-5.7
	Germacrene D-4-ol	5352847	-5.6	-6
	Isoborneol	64685	-4.6	-4.9
	Limonene	22311	-4.6	-5.3
	Linalool	6549	-4.3	-4.5
	Sabinene	18818	-4.7	-4.7

Table 1 continued

Herb	Phytoactive compounds	PubChem ID	$\Delta G$ kcal/mol	
			SARS-CoV-2 (7BTF)	SARS-CoV (6NUR)
<i>Zingiber officinalis</i>	10-Gingerdione	14440539	-5	-6.2
	10-Gingerol	168115	-5.9	-4.9
	10-Shogaol	6442612	-6.2	-5.9
	6-Dehydrogingerdione	22321203	-6	-6.8
	6-Gingerdione	162952	-5.5	-6.1
	6-Gingerol	442793	-4.8	-5
	6-Paradol	94378	-5.9	-5.2
	6-Shogaol	5281794	-6.3	-5.9
	8-Gingerol	168114	-5.1	-4.9
	8-Shogaol	6442560	-5.9	-5.8
	Zingerone	31211	-5.4	-5.6
<i>Cyperus scariosus</i>	alpha-Cyperone	6542086	-5.8	-6.5
	alpha-Pinene	6654	-4.7	-4.8
	Aristolone	165536	-6	-6.5
	beta-Patchoulene	101731	-6.2	-6.2
	beta-Pinene	14896	-4.8	-4.7
	Citral	638011	-4.3	-4.5
	Cyperene	99856	-6	-5.8
	Cyperol	14076601	-5.9	-6.4
	Isolongifolene oxide	107035	-5.9	-6
	Patchoulane	29408	-5.9	-5.7
<i>Cyperus scariosus</i>	Patchoulanol	10955174	-5.9	-5.9
	Rotundene	25203405	-6.3	-6.1
	Spathulenol	92231	-6	-6.1
	Stigmasterol	5280794	-7.3	-8.5
<i>Nigella sativa</i> seed extract	Thymoquinone	10281	-5.2	-5.4
Control	Remdesivir	121304016	-7.2	-7.5

Table 2. The predicted dissociation constant ( $K_i$ ) for binding of phytoactive compounds with target protein RdRp

Sl.No	Phytoactive constituents	Predicted Ki values ( $\mu\text{M}$ )	
		SARS CoV2 (7BTF)	SARS CoV (6NUR)
1	Withanolide D	0.239	0.144
2	Withasomniferol C	0.283	0.239
3	Withanolide A	0.336	0.202
4	Withasomniferol B	0.471	0.471
5	Withanolide E	0.471	0.398
6	Withaferin A	0.558	0.171
7	Withanolide F	0.661	0.283
8	Diosmin	0.661	0.398
9	Apigenin 7-O-b-glucuronide	0.661	0.471
10	Withanone	0.783	1.542
11	EGCG	0.783	0.558
12	Luteolin 7-O-beta-d-glucopyranoside	0.928	1.099
13	Epicatechin gallate	0.928	2.564
14	Withasomniferol A	1.099	0.928
15	Apigenin, 7-.beta.-D-glucopyranoside	1.302	2.164
16	Glycyrrhetic acid	1.542	1.099
17	beta-Amyrenone	1.542	0.661
18	beta-Amyrin	1.827	0.661
19	Withanolide B	2.164	1.827
20	Luteolin	2.164	1.302
21	Ursolic acid	2.164	2.564
22	Betulinic acid	2.164	2.564
23	Apigenin	2.564	1.827
24	oleanolic acid	2.564	1.542
25	Uvaol	2.564	3.037
26	Epigallocatechin	3.598	4.262
27	Stigmasterol	4.262	0.558
28	Ellaigic acid	5.048	0.928
29	<b>Remdesivir</b>	<b>5.048</b>	<b>3.037</b>
30	Epicatechin	9.941	5.980
31	Gallocatechin	16.525	4.262
32	10-epi gamma Eudesmol	23.188	27.468
33	Rotundene	23.188	32.539
34	Beta-patchoulene	27.468	27.468
35	Caryophyllene oxide	38.545	27.468
36	6-Dehydrogingerdione	38.545	9.941
37	Aristolone	38.545	16.525
38	Spathulenol	38.545	32.539

## Figures

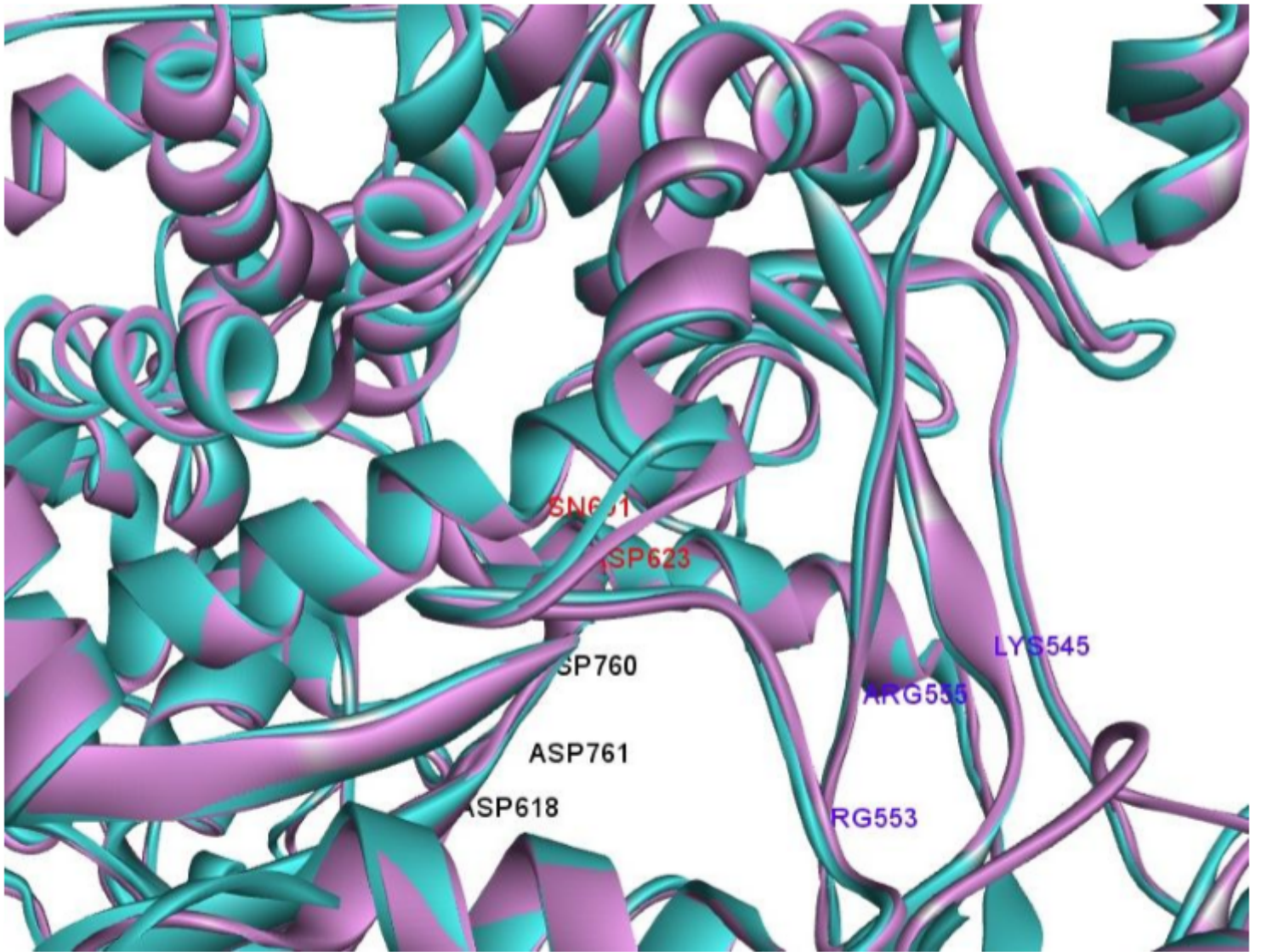


**Figure 1**

Superimposed image of nsp12 domain of 7BTF (pink ribbon) and 6NUR (cyan ribbon) with conserved amino acid residues in NTP entry site Lys545, Arg553 and Arg555 (blue label), metal ion chelating residues Asp760, Asp761 and Asp618 (black label) and NTP recognition residues Asp623 and Asn691 (red label).

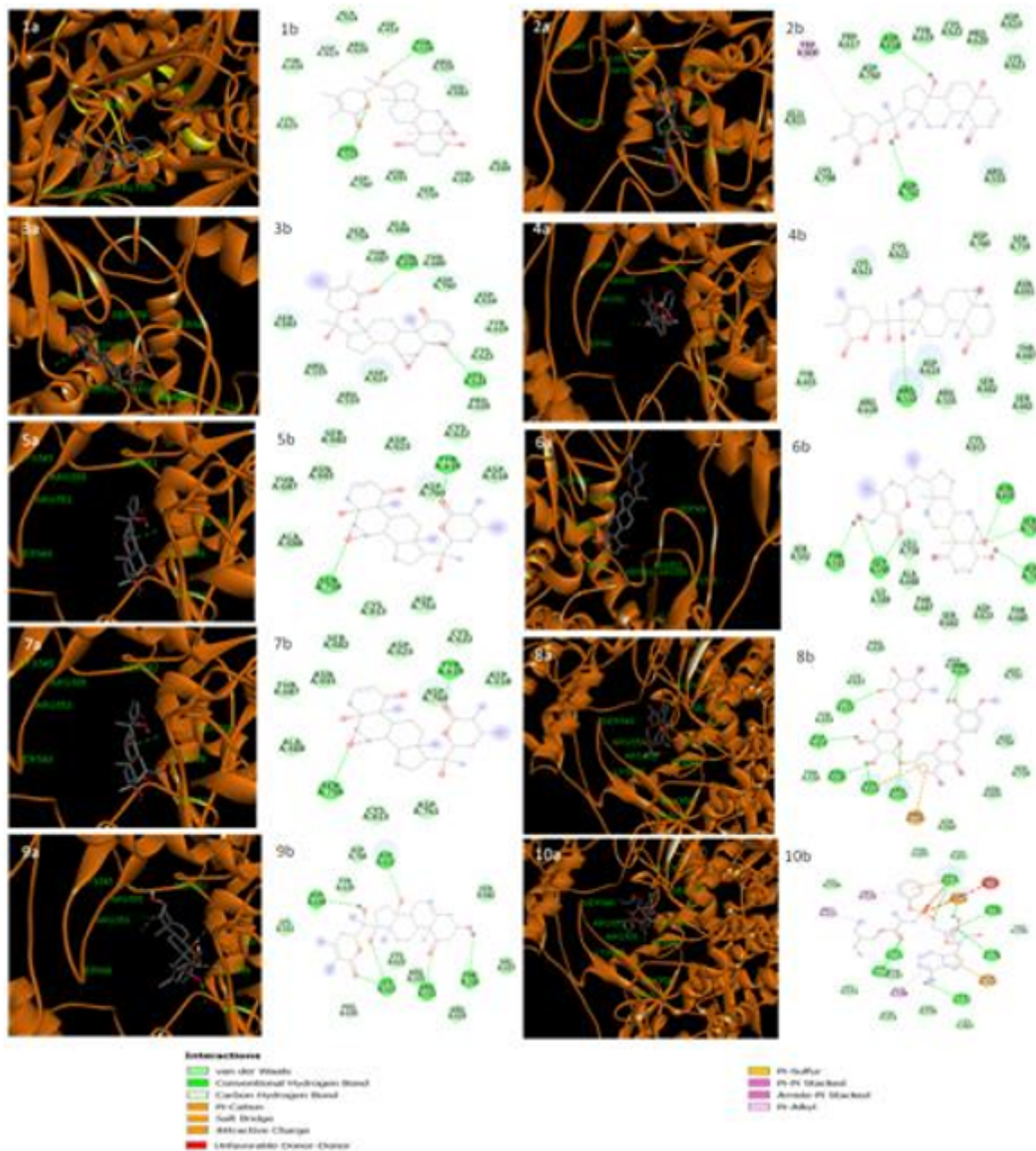


**Figure 2**

Molecular docking analysis demonstrating binding positions of various phytoactive compounds ((1) withanolide D (2) withasomniferol C (3) withanolide A (4) withanolide E (5) withasomniferol B (6) withaferin A (7) Apigenin 7-O-b-glucuronide (8) Diosmin (9) Withanolide F (10) Remdesivir) to SARS-CoV-2 RdRp (7BTF) (orange ribbon structure). The three-dimensional illustration (legend a) shows the interaction of ligands to 7BTF structure and two-dimensional diagrams (legend b) display the interactions with specific amino acid residues in the active site. The phytoactive compounds and their interacting hydrogen bonds are given in grey and green color, respectively.

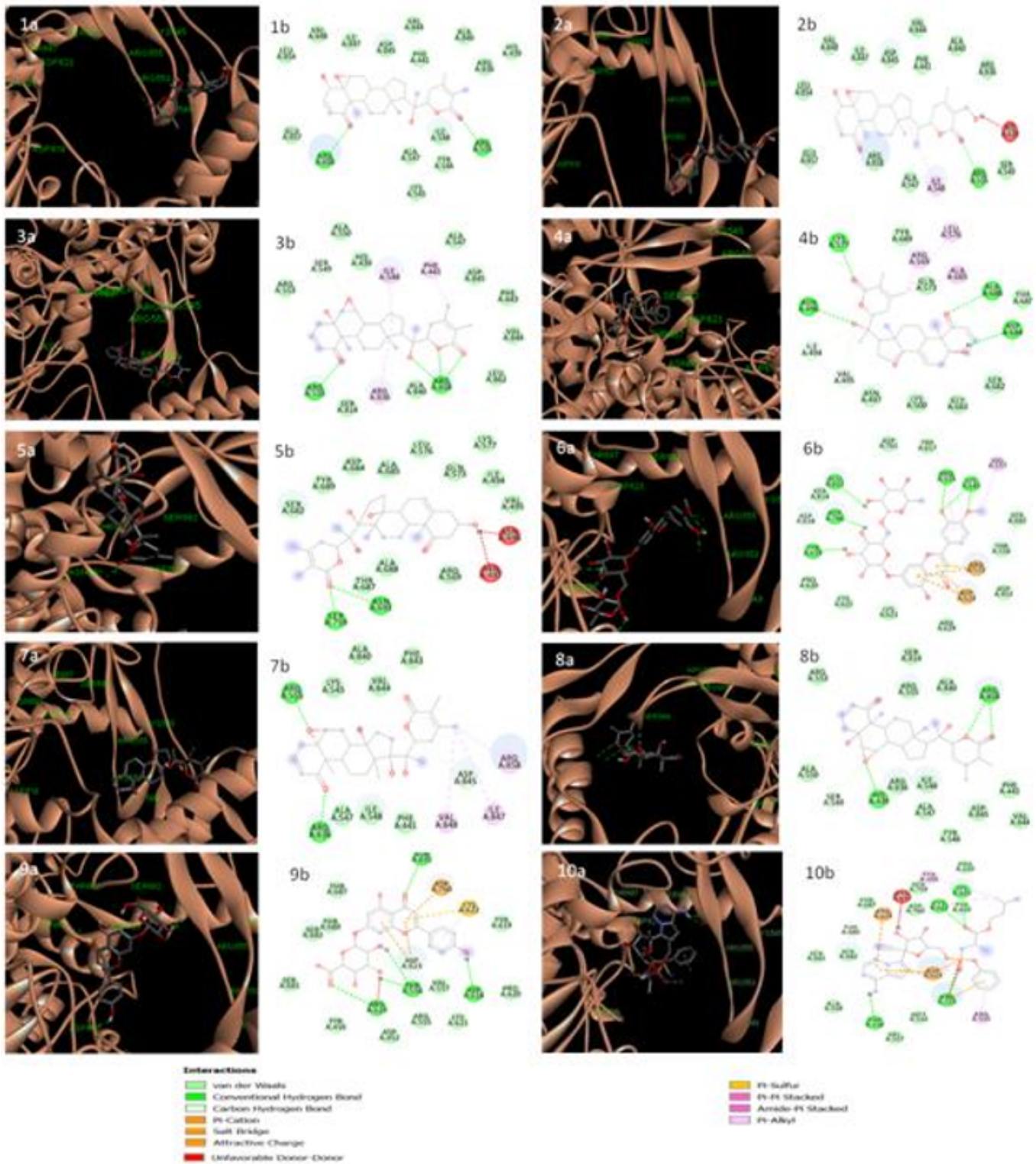


**Figure 3**

Molecular docking analysis demonstrating binding positions of various phytoactive compounds ((1) withanolide D (2) withaferin A (3) withanolide A (4) withasomniferol C (5) withanolide F (6) diosmin (7) withanolide E (8) withasomniferol B (9) apigenin 7-O-b-glucuronide (10) Remdesivir) to SARS-CoV RdRp (6NUR) (peach ribbon structure). The three-dimensional illustration (legend a) shows the interaction of ligands to 6NUR structure and two-dimensional diagrams (legend b) display the interactions with specific

amino acid residues in the active site. The phytoactive compounds and their interacting hydrogen bonds are given in grey and green color, respectively.